PROCEEDINGS OF SCIENCE

Lattice QCD at finite temperature and density: present and future

Paolo Parotto[a,*]

[a] *Pennsylvania State University, Department of Physics, University Park, PA 16802, USA*

E-mail: paolo.parotto@gmail.com

In this contribution I provide a brief overview of recent results from lattice Quantum Chromodynamics (QCD) simulations, focusing on results at finite temperature and density. In particular, I cover results obtained via analytical continuation from simulations at imaginary chemical potential. I discuss the determination of the QCD transition line, as well as the equation of state of QCD from a newly devised, alternative expansion scheme.

FAIR next generation scientists - 7th Edition Workshop (FAIRness2022)
23-27 May 2022
Paralia (Pieria, Greece)

*Speaker

PoS(FAIRness2022)042

1. Introduction

The phase diagram of QCD is a major field of investigation, from experiment and theory alike. A large body of knowledge has been gathered, that has helped paint a picture of the behavior of QCD matter at finite temperature and density. It is now known that the transition between confined and deconfined matter is a smooth crossover at around $T \sim 155 - 160\,\text{MeV}$ [1–3], and it is suggested by several model calculations [4–6] that the transition becomes first order at higher densities. The thermodynamics of the theory in the perturbative regime, namely at very large temperature and/or density, has also been described with good precision by means of resummed perturbative expansions [7]. In addition, the existence of exotic phases has been proposed at large density and low temperature [8]. From an experimental point of view, heavy-ion collisions are the best-suited tool to investigate QCD matter in different conditions. By varying the collision energy, different baryon chemical potentials can be reached in the system, allowing for a controlled exploration of the phase diagram. Comparisons of theoretical calculations to experimental measurements of particle yields and their event-by-event fluctuations have made it possible to locate in the phase diagram the so-called chemical freeze-out [9–11].

Despite this large volume of knowledge, *ab initio* information on QCD thermodynamics is in fact – strictly speaking – still limited to vanishing density and to the perturbative regime. Currently, first principle methods include perturbation theory, functional methods such as functional renormalization group (FRG) [6] and Dyson-Schwinger equations (DSE) [5], and lattice simulations.

Lattice simulations represent the primary approach to QCD thermodynamics, especially in the vicinity of the QCD transition temperature, where the coupling is strong. The lattice discretization of the euclidean theory is a natural tool for the study of equilibrium properties of QCD matter. Given sufficient computational resources, the lattice formulation provides a way to numerically solve the theory. In a few words, the lattice discretized theory allows one to calculate path integrals of the form:

$$Z\left[U,\bar{\psi},\psi\right] = \int \mathcal{D}U\,\mathcal{D}\bar{\psi}\,\mathcal{D}\psi\; e^{-S_G[U,\bar{\psi},\psi]-S_F[U,\bar{\psi},\psi]}\,, \tag{1}$$

where U are the gluon fields, $\bar{\psi},\psi$ are the fermion fields, and S_G, S_F are the gauge and fermion actions, respectively. The fermion fields can be integrated out explicitly, and the expectation value of an observable $\hat{O}$ is then:

$$\left\langle \hat{O} \right\rangle = \frac{1}{Z}\int \mathcal{D}U\,\hat{O}\,\det M[U]\,e^{-S_G[U]}\,. \tag{2}$$

These integrals are estimated on the lattice by making use of importance sampling. Instead of summing over *all* possible field configurations, a (much smaller) pool of configurations is generated with the correct probability, which is in fact the factor $\det M[U]\,e^{-S_G[U]}$. The main limitation of this approach in the study of QCD thermodynamics is the so-called fermion sign problem. When a chemical potential is introduced, the determinant $\det M[U]$ becomes complex, and cannot serve as a probability factor any longer, thus preventing the use of importance sampling, and rendering the calculations unfeasible.

Several methods have been devised to circumvent the sign problem and obtained results at finite chemical potential. Methods that directly deliver results at finite density include reweighting techniques [12–14], the complex Langevin equation [15, 16] and Lefschetz thimbles [17]. However,

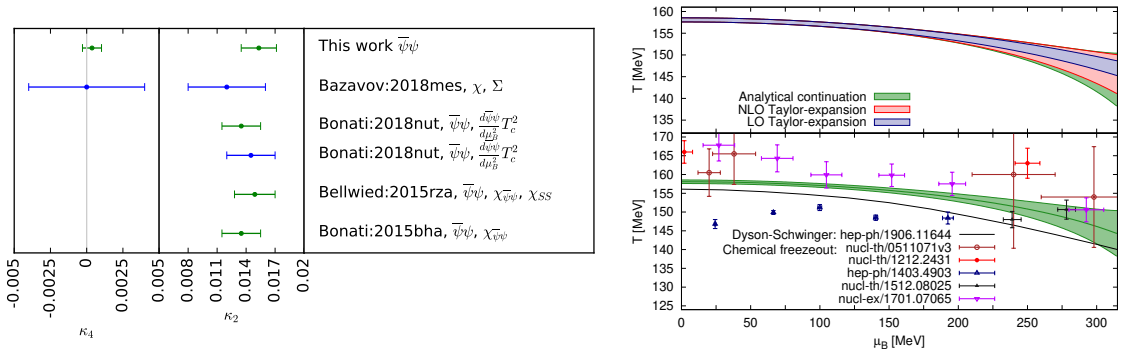

Figure 1: Left: values and errors for the κ_2 and κ_4 by different collaborations. Right: Transition line as a function of the baryon chemical potential, with and without including the next-to-leading term in the expansion. Figure from Ref. [3].

these are not yet capable of producing results on large lattices. Most results at finite density come from indirect methods, such as Taylor expansion around zero chemical potential [18–20], and analytic continuation from imaginary chemical potentials, where there is no sign problem [3, 21–24].

2. Transition line

Determing the line in the phase diagram where the chiral/deconfinement transition occurs is important both for fundamental reasons, and because of its use in modeling of heavy-ion collisions. The transition line is usually defined as an expansion around $\mu_B = 0$:

$$\frac{T_c(\mu_B)}{T_c(\mu_B = 0)} = 1 + \kappa_2 \left(\frac{\mu_B}{T_c(\mu_B)}\right)^2 + \kappa_4 \left(\frac{\mu_B}{T_c(\mu_B)}\right)^4 + O(\mu_B^6) \,, \tag{3}$$

with the curvature and hyper-curvature coefficients κ_2, κ_4 completely determining the transition line, together with the zero-density transition temperature $T_c(\mu_B = 0)$. Results for the curvature parameter κ_2 have been produced in recent years by several collaborations, both resorting to Taylor expansions and imaginary chemical potential. The first determination of κ_4 was by the HotQCD collaboration [2], which found a value compatible with zero, though with a sizeable error. This result was obtained purely with simulations at vanishing chemical potential.

In order to determine these coefficients with high precision, it is advantageous to make use of simulations at imaginary chemical potential. Because of the smallness of quark masses at the physical point, the chiral condensate $\langle\bar{\psi}\psi\rangle$ serves as a good order parameter for the QCD transition. Both the chiral condensate and the chiral susceptibility χ have been utilized to determine the transition temperature [23]:

$$\langle\bar{\psi}\psi\rangle = \frac{T}{V}\frac{\partial \ln Z}{\partial m_{ud}} \,, \qquad \chi = \frac{T}{V}\frac{\partial^2 \ln Z}{\partial m_{ud}^2} \,. \tag{4}$$

As functions of the temperature, the chiral condensate has an inflection point at the transition temperature, while the susceptibility has a peak. In Ref. [3], by considering the susceptibility as a

function of the condensate $\chi(\langle\bar{\psi}\psi\rangle)$, the transition temperature was determined for each simulated value of the chemical potential $T_c(\mu_B)$, on lattices with $N_\tau = 8, 10, 12, 16$ timeslices. Then, a combined fit in $1/N_\tau^2$ and $\hat{\mu}_B^2$ [1] yielded the desired quantities as fit parameters. The final results reached an unprecedented level of precision, as shown in the left panel of Fig.1:

$$T_c(\mu_B = 0) = 158.0(0.6)\ \text{MeV} \qquad \kappa_2 = 0.0153(18) \qquad \kappa_4 = 0.00032(67)\ . \tag{5}$$

With these results, the transition line can be drawn in the QCD phase diagram with relatively small error bars up until $\mu_B \approx 300\,\text{MeV}$, as can be seen in the right panel of Fig. 1.

3. Equation of state

Like the transition line, the equation of state of QCD at finite density is of crucial importance, both on fundamental grounds, as well as because it provides the basic information on the behavior of matter that is needed in modeling, most notably in the case of hydrodynamic simulations of heavy-ion collisions. The Taylor method has been largely employed to determine the equation of state at finite density, with coefficients up to order $O(\mu_B^8)$ available from the lattice [18, 20]. However, the expansion constructed from such coefficients presents unphysical behavior at chemical potentials $\hat{\mu}_B > 2 - 2.5$, likely because the constant-temperature extrapolation crosses the transition line at some $\hat{\mu}_B > 0$.

In Refs. [25, 26], a newly devised scheme was utilized to extrapolate the equation of state to an unprecedentedly large chemical potential of $\hat{\mu}_B = 3.5$. The starting point is that, in the vicinity of the transition temperature, many observables obey a relation of the form:

$$F(T, \hat{\mu}_B) = F(T', 0)\ , \qquad T' = T\left(1 + \kappa_2^F(T)\hat{\mu}_B^2 + \kappa_4^F(T)\hat{\mu}_B^4 + O(\hat{\mu}_B^6)\right)\ , \tag{6}$$

whereby the $\hat{\mu}_B$-dependence of the observable $F(T, \hat{\mu}_B)$ is entirely described by the parameters $\kappa_2(T)$, $\kappa_4(T)$. These are similar in nature to those in Eq. (3), which describe the $\hat{\mu}_B$-dependence of the pseudocritical temperature T_c.

Thanks to simulations at imaginary chemical potential, for a given observable F it is sufficient to determine the temperature T' satisfying Eq.(6) for each simulated value of $\hat{\mu}_B$, on each lattice, at each available temperature T. This provides a function $T'(T, \hat{\mu}_B^2, 1/N_\tau^2)$, which can be fitted to determine the coefficients $\kappa_n^F(T)$, temperature-by-temperature. The same Eq.(6) can then be used at *real* chemical potential to reconstruct the observable $F(T, \hat{\mu}_B \in \mathbb{R})$. This was done to determine thermodynamic quantities at finite chemical potential in Ref. [25] for the case with $\hat{\mu}_Q = \hat{\mu}_S = 0$, and in Ref. [26] for the case of strangeness neutrality $n_S = 0$, relevant for heavy-ion collision phenomenology. The baryon density (left) and pressure (right) in both cases are shown for chemical potentials up to $\hat{\mu}_B = 3.5$ in Fig. 2. Notably, even at such a large chemical potential there is no trace of unphysical behavior in any of the thermodynamic quantities, and the errors remain under control.

[1] We use the following notation for the dimensionless chemical potentials: $\hat{\mu}_i = \mu_i/T$.

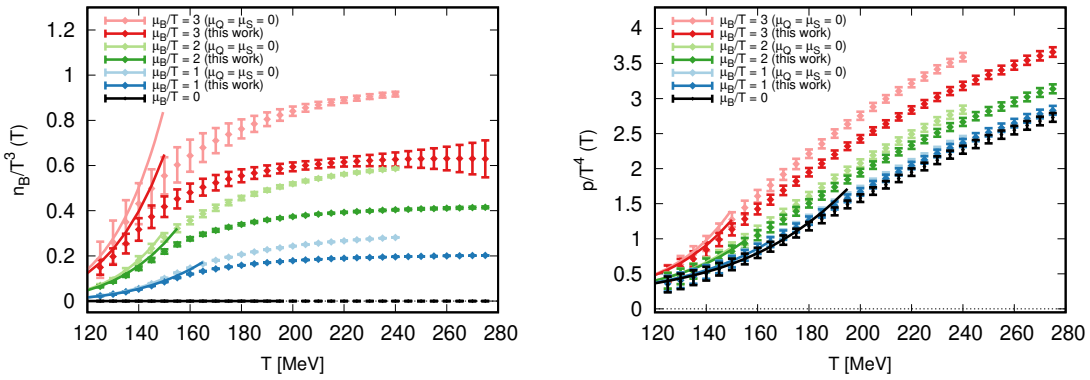

Figure 2: Baryon density and pressure up to $\hat{\mu}_B = 3.5$, in the cases without (lighter shades) and with (darker shades) strangeness neutrality.

References

[1] Y. Aoki, G. Endrodi, Z. Fodor, S.D. Katz and K.K. Szabo, *The Order of the quantum chromodynamics transition predicted by the standard model of particle physics*, *Nature* **443** (2006) 675 [hep-lat/0611014].

[2] HotQCD collaboration, *Chiral crossover in QCD at zero and non-zero chemical potentials*, *Phys. Lett. B* **795** (2019) 15 [1812.08235].

[3] S. Borsanyi, Z. Fodor, J.N. Guenther, R. Kara, S.D. Katz, P. Parotto et al., *QCD Crossover at Finite Chemical Potential from Lattice Simulations*, *Phys. Rev. Lett.* **125** (2020) 052001 [2002.02821].

[4] R. Critelli, J. Noronha, J. Noronha-Hostler, I. Portillo, C. Ratti and R. Rougemont, *Critical point in the phase diagram of primordial quark-gluon matter from black hole physics*, *Phys. Rev. D* **96** (2017) 096026 [1706.00455].

[5] P. Isserstedt, M. Buballa, C.S. Fischer and P.J. Gunkel, *Baryon number fluctuations in the QCD phase diagram from Dyson-Schwinger equations*, *Phys. Rev. D* **100** (2019) 074011 [1906.11644].

[6] F. Gao and J.M. Pawlowski, *Chiral phase structure and critical end point in QCD*, *Phys. Lett. B* **820** (2021) 136584 [2010.13705].

[7] J. Ghiglieri, A. Kurkela, M. Strickland and A. Vuorinen, *Perturbative Thermal QCD: Formalism and Applications*, *Phys. Rept.* **880** (2020) 1 [2002.10188].

[8] M.G. Alford, A. Schmitt, K. Rajagopal and T. Schäfer, *Color superconductivity in dense quark matter*, *Rev. Mod. Phys.* **80** (2008) 1455 [0709.4635].

[9] P. Alba, W. Alberico, R. Bellwied, M. Bluhm, V. Mantovani Sarti, M. Nahrgang et al., *Freeze-out conditions from net-proton and net-charge fluctuations at RHIC*, *Phys. Lett. B* **738** (2014) 305 [1403.4903].

[10] A. Andronic, P. Braun-Munzinger, K. Redlich and J. Stachel, *Decoding the phase structure of QCD via particle production at high energy*, *Nature* **561** (2018) 321 [1710.09425].

[11] R. Bellwied, J. Noronha-Hostler, P. Parotto, I. Portillo Vazquez, C. Ratti and J.M. Stafford, *Freeze-out temperature from net-kaon fluctuations at energies available at the BNL Relativistic Heavy Ion Collider*, *Phys. Rev. C* **99** (2019) 034912 [1805.00088].

[12] Z. Fodor and S.D. Katz, *A New method to study lattice QCD at finite temperature and chemical potential*, *Phys. Lett. B* **534** (2002) 87 [hep-lat/0104001].

[13] S. Borsanyi, Z. Fodor, M. Giordano, S.D. Katz, D. Nogradi, A. Pasztor et al., *Lattice simulations of the QCD chiral transition at real baryon density*, *Phys. Rev. D* **105** (2022) L051506 [2108.09213].

[14] S. Borsanyi, Z. Fodor, M. Giordano, J.N. Guenther, S.D. Katz, A. Pasztor et al., *Equation of state of a hot-and-dense quark gluon plasma: lattice simulations at real μ_B vs. extrapolations*, 2208.05398.

[15] D. Sexty, *Simulating full QCD at nonzero density using the complex Langevin equation*, *Phys. Lett. B* **729** (2014) 108 [1307.7748].

[16] M. Scherzer, E. Seiler, D. Sexty and I.O. Stamatescu, *Controlling Complex Langevin simulations of lattice models by boundary term analysis*, *Phys. Rev. D* **101** (2020) 014501 [1910.09427].

[17] AuroraScience collaboration, *New approach to the sign problem in quantum field theories: High density QCD on a Lefschetz thimble*, *Phys. Rev. D* **86** (2012) 074506 [1205.3996].

[18] S. Borsanyi, Z. Fodor, J.N. Guenther, S.K. Katz, K.K. Szabo, A. Pasztor et al., *Higher order fluctuations and correlations of conserved charges from lattice QCD*, *JHEP* **10** (2018) 205 [1805.04445].

[19] A. Bazavov et al., *Skewness, kurtosis, and the fifth and sixth order cumulants of net baryon-number distributions from lattice QCD confront high-statistics STAR data*, *Phys. Rev. D* **101** (2020) 074502 [2001.08530].

[20] HotQCD collaboration, *Taylor expansions and Padé approximants for cumulants of conserved charge fluctuations at nonvanishing chemical potentials*, *Phys. Rev. D* **105** (2022) 074511 [2202.09184].

[21] P. de Forcrand and O. Philipsen, *The QCD phase diagram for small densities from imaginary chemical potential*, *Nucl. Phys. B* **642** (2002) 290 [hep-lat/0205016].

[22] M. D'Elia and M.-P. Lombardo, *Finite density QCD via imaginary chemical potential*, *Phys. Rev. D* **67** (2003) 014505 [hep-lat/0209146].

[23] R. Bellwied, S. Borsanyi, Z. Fodor, J. Günther, S.D. Katz, C. Ratti et al., *The QCD phase diagram from analytic continuation*, *Phys. Lett. B* **751** (2015) 559 [1507.07510].

[24] C. Bonati, M. D'Elia, F. Negro, F. Sanfilippo and K. Zambello, *Curvature of the pseudocritical line in QCD: Taylor expansion matches analytic continuation*, *Phys. Rev. D* **98** (2018) 054510 [1805.02960].

[25] S. Borsányi, Z. Fodor, J.N. Guenther, R. Kara, S.D. Katz, P. Parotto et al., *Lattice QCD equation of state at finite chemical potential from an alternative expansion scheme*, *Phys. Rev. Lett.* **126** (2021) 232001 [2102.06660].

[26] S. Borsanyi, J.N. Guenther, R. Kara, Z. Fodor, P. Parotto, A. Pasztor et al., *Resummed lattice QCD equation of state at finite baryon density: Strangeness neutrality and beyond*, *Phys. Rev. D* **105** (2022) 114504 [2202.05574].